NANO LETTERS

pubs.acs.org/NanoLett

Letter

Observation of Phonon Cascades in Cu-Doped Colloidal Quantum Wells

Junhong Yu,* Sujuan Hu, Huayu Gao, Savas Delikanli, Baiquan Liu,* Jacek J. Jasieniak, Manoj Sharma,* and Hilmi Volkan Demir*

Cite This: *Nano Lett.* 2022, 22, 10224−10231

Read Online

ACCESS | Metrics & More | Article Recommendations | Supporting Information

ABSTRACT: Electronic doping has endowed colloidal quantum wells (CQWs) with unique optical and electronic properties, holding great potential for future optoelectronic device concepts. Unfortunately, how photogenerated hot carriers interact with phonons in these doped CQWs still remains an open question. Here, through investigating the emission properties, we have observed an efficient phonon cascade process (i.e., up to 27 longitudinal optical phonon replicas are revealed in the broad Cu emission band at room temperature) and identified a giant Huang−Rhys factor ($S \approx 12.4$, more than 1 order of magnitude larger than reported values of other inorganic semiconductor nanomaterials) in Cu-doped CQWs. We argue that such an ultrastrong electron−phonon coupling in Cu-doped CQWs is due to the dopant-induced lattice distortion and the dopant-enhanced density of states. These findings break the widely accepted consensus that electron−phonon coupling is typically weak in quantum-confined systems, which are crucial for optoelectronic applications of doped electronic nanomaterials.

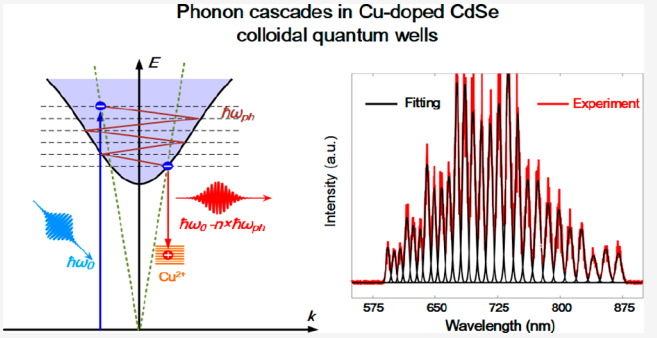

KEYWORDS: *colloidal quantum wells, copper doping, electron−phonon interactions, phonon cascades*

Colloidal quantum wells (CQWs), due to their ultranarrow emission line width,[1] giant oscillator strength,[2,3] high optical gain coefficient,[4,5] directed emission,[6,7] and solution processability,[8,9] have exhibited prominent levels of device performance in the field of optoelectronics. Recently, the incorporation of impurity transition-metal ions (e.g., Cu^{2+}, Ag^{+}, Mn^{2+}, Co^{2+} dopants) into CQWs,[10−15] which adds a new degree of freedom for manipulating optoelectronic properties different from the well-established "particle-size control" and "wave function engineering" strategies,[16,17] has been receiving considerable attention. In principle, these dopants will introduce atomic-like energy levels in the band gap of the host, prolong the excited-state lifetimes, and generate new emission bands with a large Stokes shift,[18−20] therefore holding great promise for novel device concepts. With these electronic doped CQWs, light-emitting diodes (LEDs) with tunable dual emission bands,[21,22] luminescent solar concentrators (LSCs) with high flux gain performance,[10] and other emerging optoelectronic devices with outstanding characteristics[12,18] have been demonstrated.

To further improve the optoelectronic performance of electronic doped CQWs, understanding how photogenerated hot carriers interact with phonons is of significant fundamental interest since this governs the charge mobilities,[23] the carrier cooling rate,[24] and the nonradiative decay pathway[25] and as a result determines the device's efficiency and speed. Unfortunately, possibly affected by the consensus in CQWs that electron−phonon coupling is generally weak[26,27] because of the reduced charge separation and the suppressed local electric field in quantum-confined systems (i.e., the crystal is made smaller than the Bohr radius of excitons), whether phonons can play a dominant role in the hot carrier relaxation process of electronic doped CQWs is still largely unexplored and remains as an open question. Since it has been widely reported that electronic dopants can dramatically modify electronic states and lattice configurations of the host nanocrystals,[28,29] inherent thoughts about the primary stages of carrier relaxation in electronic doped CQWs are undoubtfully inaccurate.

Here, we show that longitudinal optical (LO) phonons participate intensely in the hot carrier relaxation process of Cu-doped CdSe CQWs, evidenced by the high-order phonon cascades and a giant Huang−Rhys factor. Specifically, we have observed up to 27 periodic maxima in the copper photoluminescence (PL) emission spectrum at room temperature, in which the energy period of ∼26 meV is consistent with the LO

Received: August 29, 2022
Revised: October 26, 2022
Published: November 3, 2022

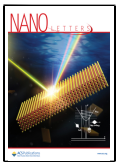

https://doi.org/10.1021/acs.nanolett.2c03427
Nano Lett. 2022, 22, 10224−10231

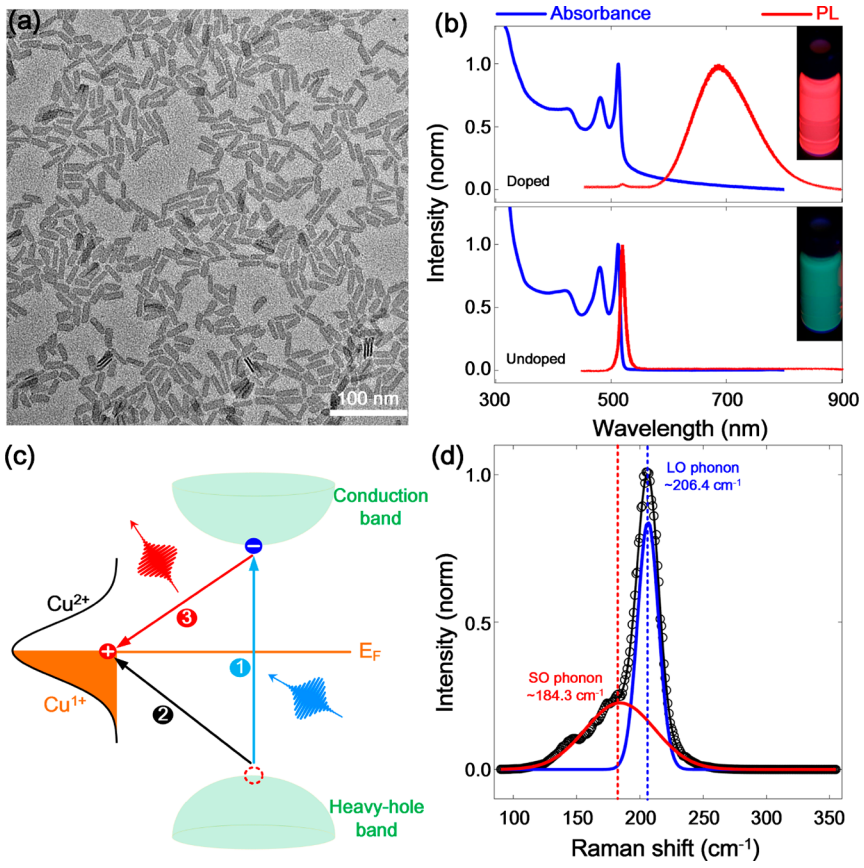

Figure 1. Basic information on Cu-doped 4 ML CdSe CQWs. (a) High angle annular dark field scanning TEM (HAADF-STEM) images of Cu-doped 4 ML CdSe CQWs (~200 copper dopants per CQW), Scale bar: 100 nm. (b) Steady-state absorbance (blue curve) and PL (red curve) spectra of Cu-doped (top panel) and undoped (bottom panel) CdSe CQWs under 355 nm continuous-wave excitations. The insets show the emission images of Cu-doped and undoped CdSe CQWs in toluene. (c) Proposed sequence of photocarrier dynamics responsible for the PL of Cu-doped CdSe CQWs. (d) Off-resonant Raman spectra of Cu-doped CdSe CQWs with an excitation of 405 nm, in which the LO and SO phonon modes can be resolved.

phonon frequency of host CQWs. Combined with the excitation energy dependence, these high-order emission replicas can be explained as phonon-assisted hot-electron transitions with a finite probability of radiative recombination at each step. By further analyzing the temperature dependence, we have deduced a giant Huang−Rhys factor of ~12.4 based on the configuration coordinate model.[30,31] These observations imply a strong electron−phonon coupling strength in Cu-doped CdSe CQWs, which we infer originates from the dopant-induced lattice distortions and atomic-like states within the forbidden energy gap. This work promotes the understanding of initial carrier−phonon interactions in electronic doped colloidal nanocrystals, which is essential for the realization of novel optoelectronic applications.

The four-monolayer (ML) Cu-doped CdSe CQWs with a quantum yield of ~80% are prepared by using a nucleation doping strategy[10,14,32,33] (details of the synthesis are shown in Figure S1). X-ray photoelectron spectroscopy (XPS) measurements are conducted to confirm the intrinsic CdSe lattice framework and the existence of Cu^{1+} dopants (see details in Figure S2). Figure 1a shows the transmission electron microscopy (TEM) image of the Cu-doped CQWs, which have an approximately rectangular shape with a uniform size distribution (lateral size: ~40 nm × ~17 nm). The average number of copper dopants per CQW ($\langle N_{Cu} \rangle$), which is determined by inductively coupled plasma mass spectrometry (ICP-MS; see details in Methods),[10,32] is about 200 in the investigated sample (i.e., ~1.2% with respect to Cu/Cd atomic concentration). Typical static absorption and PL spectra of Cu-doped and undoped CdSe CQWs under UV illumination are shown in Figure 1b: the absorbance of Cu-doped CQWs remains nearly the same compared with undoped CdSe CQWs[1,8] except that there exists a broad absorption tail on the red side of the heavy-hole excitonic feature, which is attributed to the promotion of d orbital electrons in copper dopants to the conduction band (CB) of host CQWs,[34] while the PL spectrum of Cu-doped CQWs changes dramatically and is dominated by the Cu-related emission, which peaks at ~700 nm with a huge bandwidth of ~350 meV and an ultralong lifetime of ~457 ns (see time-resolved copper emission in Figure S3).

Radiative recombination of the Cu-related emission band can be understood as follows (see Figure 1c):[35,36] copper ions introduce energy states into the forbidden gap of host CQWs, and with photoexcitation (step 1), copper dopants quickly localize the photogenerated holes in the host (step 2), Cu^{+} is promoted to Cu^{2+} and therefore activated as a radiative acceptor for the CB electrons (step 3), which can be expressed as $[Ar]3d^9 + e \rightarrow [Ar]3d^{10} + h\nu$ ($h\nu$ is the photon energy of Cu-related emission, and e denotes an electron in CB). The proposed copper emission mechanism is further supported by the sub-band-gap Cu^{+} to CB transition in the transient

https://doi.org/10.1021/acs.nanolett.2c03427
Nano Lett. 2022, 22, 10224−10231

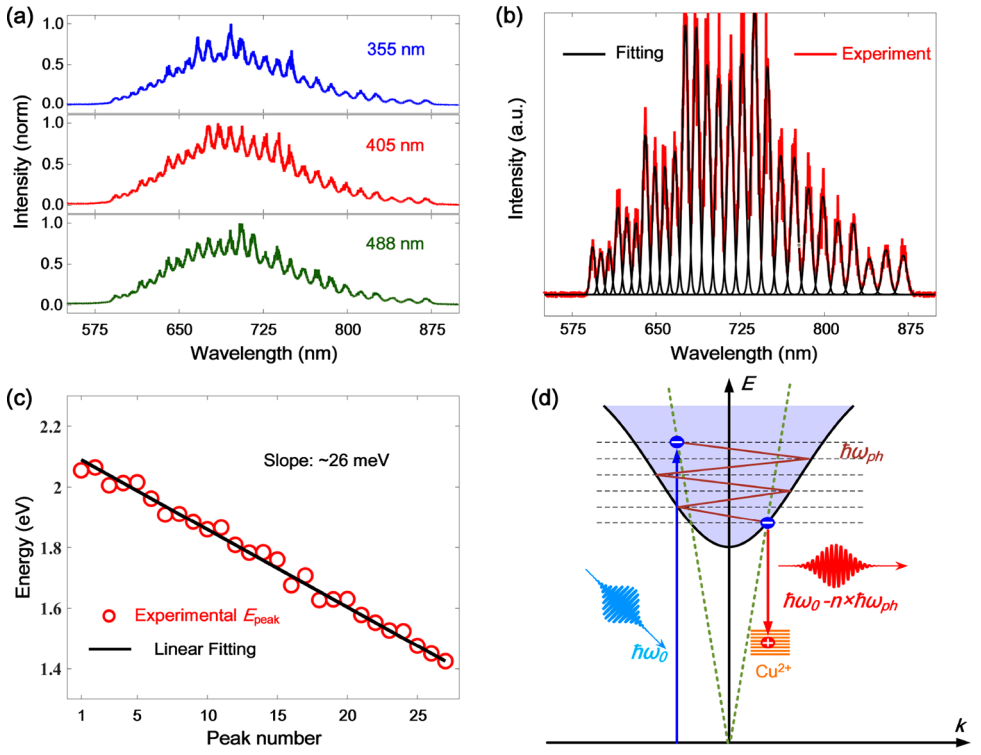

Figure 2. Room-temperature PL spectra of Cu-doped 4 ML CdSe CQWs excited with a 100 fs laser pulse (~3.2 μJ/cm^2). (a) PL spectra with three different excitation wavelengths showing similar phonon replicas. (b) Experimental multiphonon peaks with 405 nm excitations after subtracting the continuous emission profile and the corresponding Lorentz fitting. (c) Dependence of the maximum peak energy on the peak number with 405 nm excitations. A linear fitting has resolved a step energy of ~26 meV, which is highly consistent with the LO phonon energy. (d) Schematic illustration of the phonon-assisted copper emission. The phonons participating in the cascade are indicated by the brown polylines.

absorption measurement and the PL excitation (PLE) spectra (see details in Figures S4 and S5). Meanwhile, before investigating the phonon-assisted carrier relaxation, we have checked the phonon frequency in Cu-doped CQWs based on the off-resonant Raman spectrum (see experimental details in Methods). As shown in Figure 1d, the lattice vibration in Cu-doped CQWs is similar that in the undoped sample,[37,38] which consists of a dominant LO phonon peak at 206.4 cm^{-1} (25.6 meV) and a weak surface optical (SO) phonon mode related to the vibration of surface atoms.

The micro-PL of a spin-coated Cu-doped CQW film on SiO_2 substrate (thickness: ~60 nm) is recorded in reflection geometry and excited by a 100 fs laser spot (~5 μm in diameter and ~3.2 μJ/cm^2 in fluence; more experimental details are provided in Methods). Very surprisingly, we have observed that multiple strongly defined sharp peaks are superimposed on the broad Cu-emission band at room temperature. To exclude the contribution of a resonance excitation effect,[39] excitation-energy-dependent micro-PL spectra at room temperature with the same excitation intensity have been obtained. As shown in Figure 2a, if the excitation energy is higher than the heavy-hole excitonic gap of CdSe CQWs (~512 nm), similar periodic emission patterns with the same amount of peaks and the nearly fixed energy location of each peak can be identified, while with below heavy-hole excitonic gap excitations (i.e., utilizing the broad low-energy absorption tail in Figure 1b), we can only resolve a typical broad Cu-emission spectrum without any sharp emission lines (see Figure S6). Please note that the absence of a periodic emission pattern in Figure 1b is due to much lower carrier densities under continuous-wave excitations, which may cause a lower probability of multiple electron−phonon scattering processes (see details in Supplementary Note 1). Meanwhile, considering that thin-film interference could also cause periodic emission features,[40] we have measured the 405 nm excitation micro-PL of (i) a spin-coated Cu-doped CQW film on a SiO_2 substrate with a different film thickness, (ii) a spin-coated Cu-doped CQW film on a Si substrate, and (iii) a drop-casted Cu-doped CQW film on a SiO_2 substrate with a very rough surface morphology; the similar positions of peaks shown in Figures S7 and S8 indicate that our observation is not related to the multiple reflection interference effect. In addition, such a periodic emission pattern is also absent in undoped CdSe CQW films under the same excitation condition (see the measured micro-PL spectra of undoped CQW films in Figure S9). Combining these results, we preliminarily conclude that these emission replicas are linked to intrinsic relaxation mechanisms of hot electrons in the Cu-doped CdSe CQWs.

To get deeper insights into the periodic emission pattern, we have fitted all peaks between 550 and 900 nm using Gaussians[41] after subtracting the broad Cu-emission background. As shown in Figure 2b, a satisfactory approximation with a determination coefficient of >0.95 is achieved and we can roughly tell that the energy separation between two consecutive peaks is nearly constant. This observation is further confirmed by the linear dependence of energy offsets on the peak number (see Figure 2c), and its slope of ~26 meV (~209.7 cm^{-1}) shows a nice agreement with the LO phonon frequency (~206.4 cm^{-1}), implying that hot electrons are going through the single phonon mode induced cascade-like relaxation processes[42,43] in Cu-doped CQWs. As shown in

https://doi.org/10.1021/acs.nanolett.2c03427
Nano Lett. 2022, 22, 10224−10231

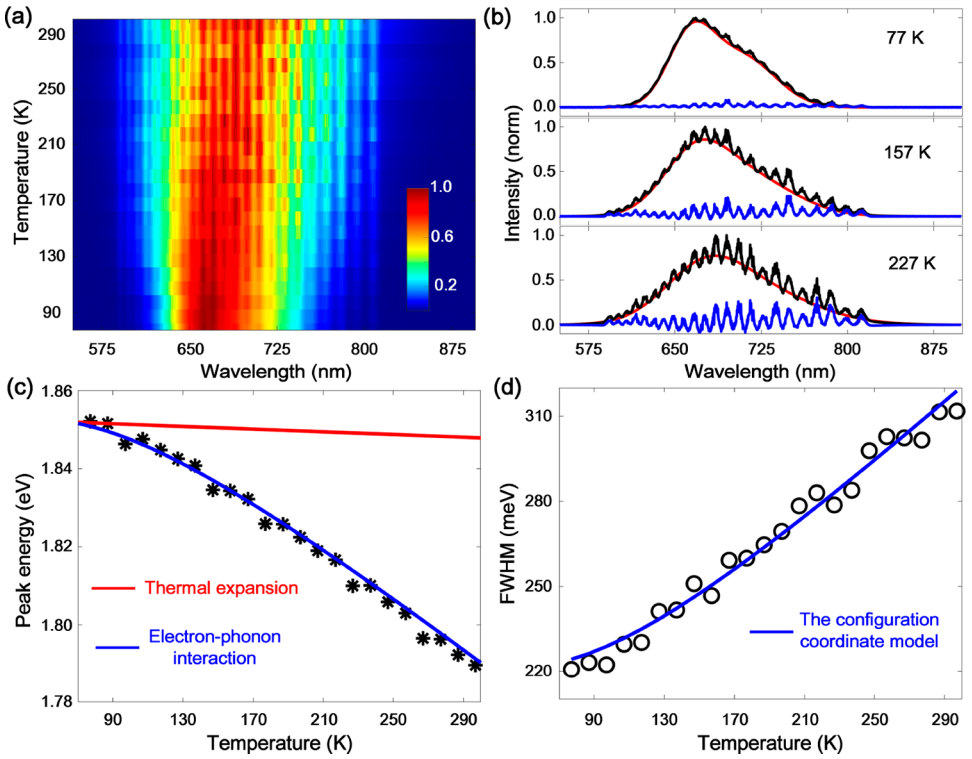

Figure 3. Temperature-dependent PL spectra of Cu-doped 4 ML CdSe CQWs with 405 nm excitation and a fluence of ~3.2 μJ/cm^2. (a) 2D PL map as a function of wavelength and temperature. (b) PL spectra at three representative temperatures. The red curve is the Gaussian line shape fitting, and the blue curve is the extracted peak profile. (c) PL peak shift with temperature. The red and blue curves indicate the individual contributions of thermal expansion and electron−phonon interaction, respectively. (d) Change in PL line width with temperature. The blue curve is a fitting according to the configuration model.

Figure 2d, this cascade process can be schematically understood as follows. With the above free-carrier gap excitation, the photogenerated electron reaches a virtual state in a well-defined in-plane wavevector cone, as indicated by the green dashed line (i.e., the wavevector $k \leq \omega/c$ in which ω is the excitation laser frequency).[44] Then hot electrons make successive transitions between real intermediate states, whereby at each step a LO phonon is emitted and radiative recombination with Cu-trapped holes can occur with a finite probability. As a result, periodic emission peaks are observed in the Cu-emission band with an energy offset equal to the LO phonon frequency.

Since temperature-dependent PL spectra are often used as important criteria to investigate electron−phonon interactions,[45] we have recorded emission profiles of Cu-doped CQWs from 77 to 297 K (the Cu-emission profile at each temperature is presented in Figures S10−S12). As shown in Figure 3a,b, the intensity of phonon replicas becomes weaker at a lower temperature (e.g., periodic peaks can be barely seen at 77 K), consistent with the fact that the strength of electron−phonon scattering is enhanced with a higher lattice temperature due to the correspondingly increased phonon thermal occupancy.[46,47] It is worth noting that in the 77−297 K temperature range we do not observe any measurable shifts in the peak position of phonon replicas, which seems to be against the phonon energy thermal modification effect.[48,49] We argue that this is because the energy shifting caused by acoustic phonons in our measured temperature range is only about 1 meV (~0.3 nm),[49] which is buried in our experimental uncertainties. Meanwhile, we have also analyzed the temperature-dependent spectral position of the broad Cu-emission band (E_{copper}) to investigate the contribution of thermal lattice expansion (TE) and electron−phonon coupling (EPC) in Cu-doped CQWs. By applying a quasi-harmonic approximation, $E_{copper}(T)$ can be represented as[50]

$$E_{copper}(T) = \text{const} + A_{TE}T + A_{EP}\left[\frac{2}{\exp(E_{phonon}/k_BT) - 1} + 1\right] \quad (1)$$

where A_{TE} and A_{EP} are the weights of TE and EPC, respectively.

Figure 3c displays fitting results of $E_{copper}(T)$ based on eq 1 with parameters of $A_{TE} = -0.017$ meV/K, $A_{EP} = -54.5$ meV, and $E_{phonon} = 25.9$ meV, from which it can be seen that (i) the extracted E_{phonon} is very close to the frequency of LO phonons, (ii) the energy matching between LO phonons and k_BT (~26 meV) at room temperature ensures its largest phonon occupancy and the dominant role in EPC processes,[51] and (iii) the overwhelming EPC implies a large electron−phonon interaction strength in Cu-doped CQWs,[52] which is further supported by analyzing the temperature-dependent line width of the broad Cu-emission band (i.e., full width at half-maximum, fwhm). Generally, the Huang−Rhys factor (S) is utilized to describe how strongly electrons are coupled to phonons, which can be calculated from fwhm(T) based on the configuration coordinate model:[30,31]

$$\text{fwhm}(T) = 2.36\sqrt{S}E_{phonon}\sqrt{\coth(E_{phonon}/2k_BT)} \quad (2)$$

From the satisfactory fitting shown in Figure 3d, we have deduced a giant Huang−Rhys factor, $S \approx 12.42$. To the best of

https://doi.org/10.1021/acs.nanolett.2c03427
Nano Lett. 2022, 22, 10224−10231

our knowledge, this is more than 1 order of magnitude larger than most reported values ($S \approx 0-1$) of other inorganic semiconductor nanostructures (such as CdSe quantum dots,[53] single-walled carbon nanotubes,[54] and single-layer transition-metal dichalcogenides[55,56]), reasonably accounting for the phonon-induced cascade hot electron relaxation process.

Following previous theoretical results in doped semiconductor nanostructures,[57−62] we infer that the strong electron−phonon interaction in Cu-doped CQWs can be attributed to the dopant-caused lattice distortions and the dopant-induced large density of states (DOS) in the forbidden band gap, as schematically recapitulated in Figure 4. It is well-known that once the Cd is partially replaced with Cu ions (see the left panel of Figure 4a), the lattice periodicity in the interior of the CQW is broken and a static Jahn−Teller distortion is favored to counter the symmetry reduction (i.e., the distortion along with T_2 Jahn−Teller nuclear coordinates; see the right panel of Figure 4a).[57] More importantly, the strong hole localization in the excited state (i.e., Cu^{2+}) implicates large nuclear distortions around Cu dopants, which could cause contraction of all copper−selenide bonds (i.e., the distortion along with the symmetric breathing local coordinate; see the right panel of Figure 4a).[58,59] These lattice distortions will cause a huge excited-state nuclear reorganization energy (E_R), which corresponds to a giant Huang−Rhys factor ($E_R = S\nu$, where ν is the lattice vibrational frequency),[57] thus rationalizing the observed strong electron−phonon interactions in Cu-doped CQWs. Furthermore, Cu dopants will induce a significant midgap DOS (see Figure 4b) into the CdSe CQW host. Based on Profeta et al.'s density functional theory calculations,[61] the trapped carriers in these introduced DOS driven by the increased electron−phonon pairing potential will strongly interact with the out-of-plane vibrations (i.e., the LO phonons) of the host lattice, thus enhancing the electron−phonon interaction.

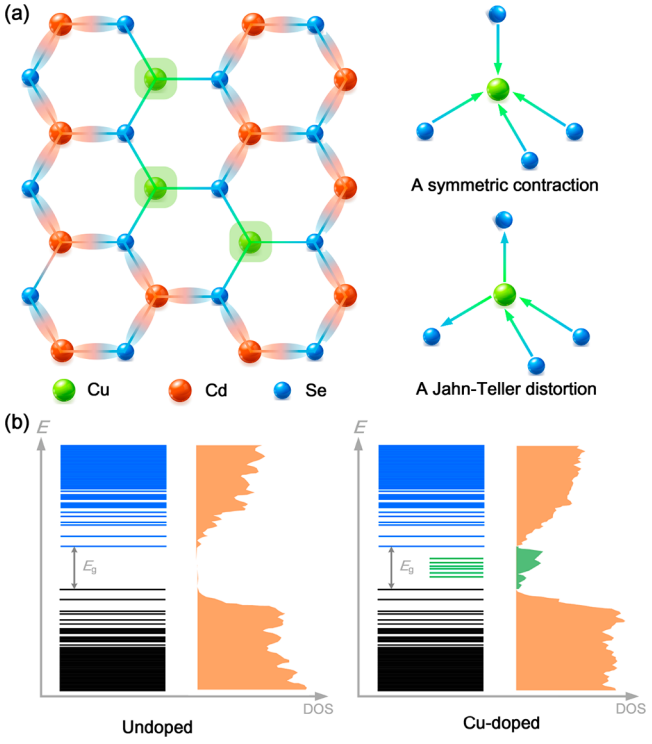

Figure 4. Possible mechanisms responsible for the strong electron−phonon interactions in Cu-doped 4 ML CdSe CQWs. (a) (left) Schematic of real space charge distributions in Cu-doped CQWs, showing carrier localization at the copper dopant. (right) Schematic of lattice distortions in Cu-doped CQWs after the carrier localization. (b) Schematic of projected density of states (DOS) in undoped and Cu-doped CQWs. Copper dopants introduce a large DOS around the Fermi level to enhance the electron−phonon interaction.

In summary, we have carried out excitation-energy- and temperature-dependent hot PL measurements in Cu-doped CdSe CQWs. Up to 27 longitudinal optical phonon replicas have been detected in the broad copper emission band at room temperature, which can be well-explained using a phonon cascade model. In addition, a giant Huang−Rhys factor ($S \approx 12.4$) is identified, which is at least 1 order of magnitude larger than previously reported values ($S \approx 0-1$) in colloidal nanocrystals. These findings indicate that an ultrastrong electron−phonon interaction plays a crucial role in the initial steps of carrier relaxation in impurity-doped CQWs, which may provide design-relevant insights for novel optoelectronic applications.

METHODS

Estimation of the Cu Atomic Level. With inductively coupled plasma mass spectrometry (ICP:MS) we estimated Cu atomic levels with respect to cadmium and selenium. The average dimensions of our 4 ML copper-doped CdSe CQWs measured by TEM microscopy are $(40.3 \pm 1.6) \times (17.3 \pm 2.9) \times 1.2$ nm, which suggests ∼17430 cadmium and ∼13695 selenium atoms in one CQW. Therefore, using ICP:MS measurements, we can estimate Cu atoms per CQW.

Off-Resonant Raman spectroscopy. The room-temperature Raman spectra of the Cu-doped CQWs were obtained using a micro-Raman spectrometer (50× objective lens with an NA value of 0.75 and a spectral resolution of around 1 cm^{-1}) in the backscattering geometry. A linearly polarized argon ion laser (488 nm) was used as an excitation light source. The focused excitation spot size was about 5 μm in diameter, and the on-sample excitation fluence was controlled by a neutral-density filter to a very low value (0.1 $\mu J/cm^2$) to avoid any irreversible thermal degradation of the samples.

Micro-PL Spectra Measurements. The excitation pulse was generated from an optical parametric amplifier (Light Conversion TOPAS-C) which was pumped by a 1 kHz regenerative amplifier (80 fs, 1 kHz, 800 nm). The excitation pulse was focused on the sample surface via a 50× objective lens (numerical aperture 0.45), and the PL spectra were recorded by a fiber-coupled ANDOR spectrometer with a CCD detector. The focused excitation spot size was about 5 μm in diameter, and the on-sample excitation fluence was controlled by the neutral-density filter. For the low-temperature micro-PL measurement, the sample was cooled with a liquid nitrogen cryostat.

ASSOCIATED CONTENT

Supporting Information

The Supporting Information is available free of charge at https://pubs.acs.org/doi/10.1021/acs.nanolett.2c03427.

Synthetic details, estimation of electron−phonon scattering probability, X-ray photoelectron spectroscopy, time-resolved copper emission dynamics, transient absorption spectroscopy, photoluminescence excitation spectroscopy, micro-PL spectra of Cu-doped and

https://doi.org/10.1021/acs.nanolett.2c03427
Nano Lett. 2022, 22, 10224−10231

undoped CQW films on different substrates with different thicknesses, and temperature-dependent copper emission spectra (PDF)

AUTHOR INFORMATION

Corresponding Authors

Junhong Yu − *Laboratory for Shock Wave and Detonation Physics, Institute of Fluid Physics, China Academy of Engineering Physics, Mianyang 621900, People's Republic of China; LUMINOUS! Centre of Excellence for Semiconductor Lighting and Displays, School of Electrical and Electronic Engineering, Nanyang Technological University, Singapore 639798, Singapore;* orcid.org/0000-0001-6136-552X; Email: jyu012@e.ntu.edu.sg

Baiquan Liu − *School of Electronics and Information Technology, Sun Yat-sen University, Guangzhou 510275, People's Republic of China;* orcid.org/0000-0001-9375-7683; Email: liubq33@mail.sysu.edu.cn

Manoj Sharma − *LUMINOUS! Centre of Excellence for Semiconductor Lighting and Displays, School of Electrical and Electronic Engineering, Nanyang Technological University, Singapore 639798, Singapore; ARC Centre of Excellence in Exciton Science, Department of Materials Science and Engineering, Monash University, Melbourne, Victoria 3800, Australia;* orcid.org/0000-0001-5215-9740; Email: manoj.sharma@monash.edu

Hilmi Volkan Demir − *LUMINOUS! Centre of Excellence for Semiconductor Lighting and Displays, School of Electrical and Electronic Engineering, Nanyang Technological University, Singapore 639798, Singapore; Department of Electrical and Electronics Engineering and Department of Physics, UNAM-Institute of Materials Science and Nanotechnology, Bilkent University, Bilkent, Ankara 06800, Turkey; School of Physical and Mathematical Sciences, Division of Physics and Applied Physics, Nanyang Technological University, Singapore 639798, Singapore;* orcid.org/0000-0003-1793-112X; Email: volkan@fen.bilkent.edu.tr

Authors

Sujuan Hu − *School of Electronics and Information Technology, Sun Yat-sen University, Guangzhou 510275, People's Republic of China*

Huayu Gao − *School of Electronics and Information Technology, Sun Yat-sen University, Guangzhou 510275, People's Republic of China*

Savas Delikanli − *Department of Electrical and Electronics Engineering and Department of Physics, UNAM-Institute of Materials Science and Nanotechnology, Bilkent University, Bilkent, Ankara 06800, Turkey;* orcid.org/0000-0002-0613-8014

Jacek J. Jasieniak − *ARC Centre of Excellence in Exciton Science, Department of Materials Science and Engineering, Monash University, Melbourne, Victoria 3800, Australia;* orcid.org/0000-0002-1608-6860

Complete contact information is available at: https://pubs.acs.org/10.1021/acs.nanolett.2c03427

Notes

The authors declare no competing financial interest.

ACKNOWLEDGMENTS

B.L. acknowledges financial support from the National Natural Science Foundation of China under Grant 62104265, the Science and Technology Program of Guangdong Province under Grant 2021A0505110009, and the Innovation and Technology Fund under Grant GHP/006/20GD. M.S. and J.J.J. acknowledge funding through the Australian Research Council Center of Excellence in Exciton Science (Grant No. CE170100026). H.V.D. acknowledges financial support in part from the Singapore Agency for Science, Technology and Research (A*STAR) MTC program under grant number M21J9b0085, Ministry of Education, Singapore, under its Academic Research Fund Tier 1 (MOE-RG62/20) and in part from TUBITAK 119N343, 20AG001, 121N395, and 121C266. H.V.D. also acknowledges support from TUBA and TUBITAK 2247-A National Leader Researchers Program (121C266).

REFERENCES

(1) Ithurria, S.; Tessier, M. D.; Mahler, B.; Lobo, R. P. S. M.; Dubertret, B.; Efros, A. L. Colloidal Nanoplatelets with Two-Dimensional Electronic Structure. *Nat. Mater.* **2011**, *10*, 936−941.

(2) Geiregat, P.; Rodá, C.; Tanghe, I.; et al. Localization-limited exciton oscillator strength in colloidal CdSe nanoplatelets revealed by the optically induced stark effect. *Light: Sci. Appl.* **2021**, *10*, 112.

(3) Yu, J.; Hou, S.; Sharma, M.; et al. Strong Plasmon-Wannier Mott Exciton Interaction with High Aspect Ratio Colloidal Quantum Wells. *Matter* **2020**, *2*, 1550.

(4) Guzelturk, B.; Pelton, M.; Olutas, M.; Demir, H. V. Giant Modal Gain Coefficients in Colloidal II−VI Nanoplatelets. *Nano Lett.* **2019**, *19* (1), 277−282.

(5) Yu, J.; Sharma, M.; Sharma, A.; Delikanli, S.; Demir, H. V.; Dang, C. All-optical control of exciton flow in a colloidal quantum well complex. *Light: Sci. Appl.* **2020**, *9*, 27.

(6) Gao, Y.; Weidman, M. C.; Tisdale, W. A. CdSe Nanoplatelet Films with Controlled Orientation of Their Transition Dipole Moment. *Nano Lett.* **2017**, *17*, 3837−3843.

(7) Scott, R.; Heckmann, J.; Prudnikau, A. V.; Antanovich, A.; Mikhailov, A.; Owschimikow, N.; Artemyev, M.; Climente, J. I.; Woggon, U.; Grosse, N. B.; Achtstein, A. W. Directed Emission of CdSe Nanoplatelets Originating from Strongly Anisotropic 2D Electronic Structure. *Nat. Nanotechnol.* **2017**, *12*, 1155−1160.

(8) Ithurria, S.; Bousquet, G.; Dubertret, B. Continuous Transition from 3D to 1D Confinement Observed during the Formation of CdSe Nanoplatelets. *J. Am. Chem. Soc.* **2011**, *133* (9), 3070−3077.

(9) Yu, J.; Dang, C. Colloidal Metal Chalcogenide Quantum Wells for Laser Applications. *Cell Rep. Phys. Sci.* **2021**, *2*, 100308.

(10) Sharma, M.; Gungor, K.; Yeltik, A.; Olutas, M.; Guzelturk, B.; Kelestemur, Y.; Erdem, T.; Delikanli, S.; McBride, J. R.; Demir, H. V. Near-Unity Emitting Copper-Doped Colloidal Semiconductor Quantum Wells for Luminescent Solar Concentrators. *Adv. Mater.* **2017**, *29*, 1700821.

(11) Yu, J.; Sharma, M.; Delikanli, S.; Birowosuto, M. D.; Demir, H. V.; Dang, C. Mutual Energy Transfer in a Binary Colloidal Quantum Well Complex. *J. Phys. Chem. Lett.* **2019**, *10*, 5193−5199.

(12) Sharma, M.; Delikanli, S.; Demir, H. V. Two-Dimensional CdSe-Based Nanoplatelets: Their Heterostructures, Doping, Photophysical Properties, and Applications. *Proceedings of the IEEE* **2020**, *108*, 655−675.

(13) Yu, J.; Sharma, M.; Wang, Y.; Delikanli, S.; Baruj, H. D.; Sharma, A.; Demir, H. V.; Dang, C. Modulating Emission Properties in a Host−Guest Colloidal Quantum Well Superlattice. *Adv. Optical Mater.* **2022**, *10*, 2101756.

(14) Sharma, M.; Olutas, M.; Yeltik, A.; Kelestemur, Y.; Sharma, A.; Delikanli, S.; Guzelturk, B.; Gungor, K.; McBride, J. R.; Demir, H. V. Understanding the Journey of Dopant Copper Ions in Atomically Flat Colloidal Nanocrystals of CdSe Nanoplatelets Using Partial Cation Exchange Reactions. *Chem. Mater.* **2018**, *30*, 3265−3275.

(15) Khan, A. H.; Pinchetti, V.; Tanghe, I.; Dang, Z.; Martín-García, B.; Hens, Z.; Van Thourhout, D.; Geiregat, P.; Brovelli, S.; Moreels, I. Tunable and Efficient Red to Near-Infrared Photoluminescence by Synergistic Exploitation of Core and Surface Silver Doping of CdSe Nanoplatelets. *Chem. Mater.* **2019**, *31*, 1450−1459.
(16) Brovelli, S.; Schaller, R. D.; Crooker, S. A.; García-Santamaría, F.; Chen, Y.; Viswanatha, R.; Hollingsworth, J. A.; Htoon, H.; Klimov, V. I. Nano-Engineered Electron−Hole Exchange Interaction Controls Exciton Dynamics in Core−Shell Semiconductor Nanocrystals. *Nat. Commun.* **2011**, *2*, 280.
(17) Bae, W. K.; Padilha, L. A.; Park, Y.-S.; McDaniel, H.; Robel, I.; Pietryga, J. M.; Klimov, V. I. Controlled Alloying of the Core−Shell Interface in CdSe/CdS Quantum Dots for Suppression of Auger Recombination. *ACS Nano* **2013**, *7*, 3411−3419.
(18) Brovelli, S.; Galland, C.; Viswanatha, R.; Klimov, V. I. Tuning Radiative Recombination in Cu-Doped Nanocrystals via Electrochemical Control of Surface Trapping. *Nano Lett.* **2012**, *12*, 4372−4379.
(19) Hughes, K. E.; Hartstein, K. H.; Gamelin, D. R. Photodoping and Transient Spectroscopies of Copper-Doped CdSe/CdS Nanocrystals. *ACS Nano* **2018**, *12*, 718−728.
(20) Whitham, P. J.; Knowles, K. E.; Reid, P. J.; Gamelin, D. R. Photoluminescence Blinking and Reversible Electron Trapping in Copper-Doped CdSe Nanocrystals. *Nano Lett.* **2015**, *15*, 4045−4051.
(21) Liu, B.; Sharma, M.; Yu, J.; Shendre, S.; Hettiarachchi, C.; Sharma, A.; Yeltik, A.; Wang, L.; Sun, H.; Dang, C.; Demir, H. V. Light-Emitting Diodes with Cu-Doped Colloidal Quantum Wells: From Ultrapure Green, Tunable Dual-Emission to White Light. *Small* **2019**, *15*, No. 1901983.
(22) Liu, B.; Sharma, M.; Yu, J.; Wang, L.; Shendre, S.; Sharma, A.; Izmir, M.; Delikanli, S.; Yeltik, A.; Dang, C.; Sun, H.; Demir, H. V. Management of electroluminescence from silver-doped colloidal quantum well light-emitting diodes. *Cell Rep. Phys. Sci.* **2022**, *3*, 100860.
(23) Jasrasaria, D.; Rabani, E. Interplay of Surface and Interior Modes in Exciton-Phonon Coupling at the Nanoscale. *Nano Lett.* **2021**, *21*, 8741−8748.
(24) Achtstein, A. W.; Schliwa, A.; Prudnikau, A.; Hardzei, M.; Artemyev, M. V.; Thomsen, C.; Woggon, U. Electronic Structure and Exciton-Phonon Interaction in Two-Dimensional Colloidal Cdse Nanosheets. *Nano Lett.* **2012**, *12* (6), 3151−3157.
(25) Pelton, M.; Ithurria, S.; Schaller, R. D.; Dolzhnikov, D. S.; Talapin, D. V. Carrier cooling in colloidal quantum wells. *Nano Lett.* **2012**, *12*, 6158−6163.
(26) Lin, C.; Gong, K.; Kelley, D. F.; Kelley, A. M. Size-Dependent Exciton−Phonon Coupling in CdSe Nanocrystals through Resonance Raman Excitation Profile Analysis. *J. Phys. Chem. C* **2015**, *119*, 7491−7498.
(27) Achtstein, A. W.; Marquardt, O.; Scott, R.; Ibrahim, M.; Riedl, T.; Prudnikau, A. V.; Antanovich, A.; Owschimikow, N.; Lindner, J. K.; Artemyev, M.; et al. Impact of Shell Growth on Recombination Dynamics and Exciton−Phonon Interaction in CdSe−CdS Core−Shell Nanoplatelets. *ACS Nano* **2018**, *12*, 9476−9483.
(28) Nelson, H. D.; Li, X.; Gamelin, D. R. Computational Studies of the Electronic Structures of Copper-Doped CdSe Nanocrystals: Oxidation States, Jahn−Teller Distortions, Vibronic Bandshapes, and Singlet−Triplet Splittings. *J. Phys. Chem. C* **2016**, *120*, 5714−5723.
(29) Knowles, K. E.; Nelson, H. D.; Kilburn, T. B.; Gamelin, D. R. Singlet−Triplet Splittings in the Luminescent Excited States of Colloidal Cu^+:CdSe, Cu^+:InP, and $CuInS_2$ Nanocrystals: Charge-Transfer Configurations and Self-Trapped Excitons. *J. Am. Chem. Soc.* **2015**, *137*, 13138−13147.
(30) Stadler, W.; Hofmann, D. M.; Alt, H. C.; Muschik, T.; Meyer, B. K.; Weigel, E.; Müller-Vogt, G.; Salk, M.; Rupp, E.; Benz, K. W. Optical investigations of defects in $Cd_{1-x}Zn_xTe$. *Phys. Rev. B* **1995**, *51*, 10619−10630.
(31) Wang, L.; Zheng, W.; Vitale, F.; Zhang, X.; Li, X.; Ji, Y.; Liu, Z.; Ghaebi, O.; Plass, C. T.; Domes, R.; Frosch, T.; Soavi, G.; Wendler, E.; Zhang, Y.; Ronning, C. Wide-Bandgap Double Perovskites with Multiple Longitudinal-Optical Phonon Scattering. *Adv. Funct. Mater.* **2022**, *32*, 2111338.
(32) Yu, J.; Sharma, M.; Li, M.; Delikanli, S.; Sharma, A.; Taimoor, M.; Altintas, Y.; McBride, J. R.; Kusserow, T.; Sum, T. C.; Demir, H. V.; Dang, C. Low-Threshold Lasing from Copper-Doped CdSe Colloidal Quantum Wells. *Laser Photonics Rev.* **2021**, *15*, 2100034.
(33) Yu, J.; Sharma, M.; Li, M.; Liu, B.; Hernandez-Martinez, P. L.; Delikanli, S.; Sharma, A.; Altintas, Y.; Hettiarachchi, C.; Sum, T. C.; Demir, H. V.; Dang, C. Efficient generation of emissive many-body correlations in copper-doped colloidal quantum wells. *Cell Rep. Phys. Sci.* **2022**, 3 (9), 101049.
(34) Hughes, K. E.; Hartstein, K. H.; Gamelin, D. R. Photodoping and Transient Spectroscopies of Copper-Doped CdSe/CdS Nanocrystals. *ACS Nano* **2018**, *12*, 718−728.
(35) Pinchetti, V.; Di, Q.; Lorenzon, M.; Camellini, A.; Fasoli, M.; Zavelani-Rossi, M.; Meinardi, F.; Zhang, J.; Crooker, S. A.; Brovelli, S. Excitonic Pathway to Photoinduced Magnetism in Colloidal Nanocrystals with Nonmagnetic Dopants. *Nat. Nanotechnol.* **2018**, *13*, 145−151.
(36) van der Stam, W.; de Graaf, M.; Gudjonsdottir, S.; Geuchies, J. J.; Dijkema, J. J.; Kirkwood, N.; Evers, W. H.; Longo, A.; Houtepen, A. J. Tuning and Probing the Distribution of Cu^+ and Cu^{2+} Trap States Responsible for Broad-Band Photoluminescence in CuInS2 Nanocrystals. *ACS Nano* **2018**, *12*, 11244−11253.
(37) Cherevkov, S. A.; Fedorov, A. V.; Artemyev, M. V.; Prudnikau, A. V.; Baranov, A. V. Anisotropy of Electron-Phonon Interaction in Nanoscale CdSe Platelets as Seen via Off-Resonant and Resonant Raman Spectroscopy. *Phys. Rev. B* **2013**, *88*, No. 041303.
(38) Sigle, D. O.; Hugall, J. T.; Ithurria, S.; Dubertret, B.; Baumberg, J. J. Probing confined phonon modes in individual CdSe nanoplatelets using surface-enhanced Raman scattering. *Phys. Rev. Lett.* **2014**, *113*, No. 087402.
(39) Paradisanos, I.; Wang, G.; Alexeev, E. M.; Cadore, A. R.; Marie, X.; Ferrari, A. C.; Glazov, M. M.; Urbaszek, B. Efficient Phonon Cascades in WSe2Monolayers. *Nat. Commun.* **2021**, *12*, 538.
(40) Larsen, J. K.; Li, S.-Y.; Scragg, J. J. S.; Ren, Y.; Hägglund, C.; Heinemann, M. D.; Kretzschmar, S.; Unold, T.; Platzer-Björkman, C. Interference Effects in Photoluminescence Spectra of Cu_2ZnSnS_4 and $Cu(In,Ga)Se_2$ Thin Films. *J. Appl. Phys.* **2015**, *118*, No. 035307.
(41) Vokhmintsev, A.; Weinstein, I.; Zamyatin, D. Electron-phonon interactions in subband excited photoluminescence of hexagonal boron nitride. *J. Lumin.* **2019**, *208*, 208−363.
(42) Gross, E.; Permogorov, S.; Morozenko, Y.; Kharlamov, B. Hot-Exciton Luminescence in CdSe Crystals. *Phys. Stat. Sol. B* **1973**, *59*, 551−560.
(43) Shi, S. L.; Li, G. Q.; Xu, S. J.; Zhao, Y.; Chen, G. H. Green Luminescence Band in ZnO: Fine Structures, Electron−Phonon Coupling, and Temperature Effect. *J. Phys. Chem. B* **2006**, *110*, 10475−10478.
(44) Yu, J.; Shendre, S.; Koh, W.-k.; Liu, B.; Li, M.; Hou, S.; Hettiarachchi, C.; Delikanli, S.; Hernandez-Martínez, P.; Birowosuto, M. D.; Wang, H.; Sum, T.; Demir, H. V.; Dang, C. Electrically Control Amplified Spontaneous Emission in Colloidal Quantum Dots. *Sci. Adv.* **2019**, *5*, No. eaav3140.
(45) Achtstein, A. W.; Schliwa, A.; Prudnikau, A.; Hardzei, M.; Artemyev, M. V.; Thomsen, C.; Woggon, U. Electronic Structure and Exciton − Phonon Interaction in Two- Dimensional Colloidal CdSe Nanosheets. *Nano Lett.* **2012**, *12*, 3151−3157.
(46) Zhang, Q.; Zhang, J.; Utama, M. I. B.; Peng, B.; de la Mata, M.; Arbiol, J.; Xiong, Q. Exciton-phonon coupling in individual ZnTe nanorods studied by resonant Raman spectroscopy. *Phys. Rev. B: Condens. Matter Mater. Phys.* **2012**, *85*, No. 085418.
(47) Beechem, T.; Graham, S. Temperature and doping dependence of phonon lifetimes and decay pathways in GaN. *J. Appl. Phys.* **2008**, *103*, 093507.
(48) Zhu, S.; Zheng, W. Temperature-Dependent Phonon Shifts in van der Waals Crystals. *J. Phys. Chem. Lett.* **2021**, *12* (22), 5261−5270.

https://doi.org/10.1021/acs.nanolett.2c03427
Nano Lett. 2022, 22, 10224−10231

(49) Scott, R.; Prudnikau, A. V.; Antanovich, A.; Christodoulou, S.; Riedl, T.; Bertrand, G. H. V.; Owschimikow, N.; Lindner, J. K. N.; Hens, Z.; Moreels, I.; et al. A Comparative Study Demonstrates Strong Size Tunability of Carrier-Phonon Coupling in CdSe-Based 2d and 0d Nanocrystals. *Nanoscale* **2019**, *11*, 3958−3967.
(50) Paritmongkol, W.; Powers, E. R.; Dahod, N. S.; Tisdale, W. A. Two Origins of Broadband Emission in Multilayered 2D Lead Iodide Perovskites. *J. Phys. Chem. Lett.* **2020**, *11* (20), 8565−8572.
(51) Cheng, L.; Zhu, Y.; Wang, W.; Zheng, W. Strong Electron-Phonon Coupling in β-Ga_2O_3: A Huge Broadening of Self-Trapped Exciton Emission and a Significant Red Shift of the Direct Bandgap. *J. Phys. Chem. Lett.* **2022**, *13* (13), 3053−3058.
(52) Gramlich, M.; Lampe, C.; Drewniok, J.; Urban, A. S. How Exciton−Phonon Coupling Impacts Photoluminescence in Halide Perovskite Nanoplatelets. *J. Phys. Chem. Lett.* **2021**, *12*, 11371−11377.
(53) Dong, S.; Trivedi, D.; Chakrabortty, S.; Kobayashi, T.; Chan, Y.; Prezhdo, O. V.; Loh, Z. H. Observation of an Excitonic Quantum Coherence in CdSe Nanocrystals. *Nano Lett.* **2015**, *15* (10), 6875−82.
(54) Lueer, L.; Gadermaier, C.; Crochet, J.; Hertel, T.; Brida, D.; Lanzani, G. Coherent Phonon Dynamics in Semiconducting Carbon Nanotubes: A Quantitative Study of Electron-Phonon Coupling. *Phys. Rev. Lett.* **2009**, *102*, 127401.
(55) Li, D.; Trovatello, C.; Dal Conte, S.; Nuß, M.; Soavi, G.; Wang, G.; Ferrari, A. C.; Cerullo, G.; Brixner, T. Exciton-Phonon Coupling Strength in Single-Layer MoSe2 at Room Temperature. *Nat. Commun.* **2021**, *12*, 954.
(56) Zhang, Q.; Liu, X.; Utama, M. I. B.; Zhang, J.; de la Mata, M.; Arbiol, J.; Lu, Y.; Sum, T. C.; Xiong, Q. Highly enhanced exciton recombination rate by strong electron−phonon coupling in single ZnTe nanobelt. *Nano Lett.* **2012**, *12*, 6420−6427.
(57) Nelson, H. D.; Gamelin, D. R. Valence-Band Electronic Structures of Cu^+-Doped ZnS, Alloyed Cu−In−Zn−S, and Ternary $CuInS_2$ Nanocrystals: A Unified Description of Photoluminescence across Compositions. *J. Phys. Chem. C* **2018**, *122*, 18124−18133.
(58) Nelson, H. D.; Hinterding, S. O. M.; Fainblat, R.; Creutz, S. E.; Li, X.; Gamelin, D. R. Mid-Gap States and Normal vs Inverted Bonding in Luminescent Cu^+- and Ag^+-Doped CdSe Nanocrystals. *J. Am. Chem. Soc.* **2017**, *139*, 6411−6421.
(59) Feldmann, S.; Gangishetty, M. K.; Bravić, I.; Neumann, T.; Peng, B.; Winkler, T.; Friend, R. H.; Monserrat, B.; Congreve, D. N.; Deschler, F. Charge Carrier Localization in Doped Perovskite Nanocrystals Enhances Radiative Recombination. *J. Am. Chem. Soc.* **2021**, *143*, 8647.
(60) Si, C.; Liu, Z.; Duan, W. H.; Liu, F. First-Principles Calculations on the Effect of Doping and Biaxial Tensile Strain on Electron-Phonon Coupling in Graphene. *Phys. Rev. Lett.* **2013**, *111*, 196802.
(61) Profeta, G.; Calandra, M.; Mauri, F. Phonon-mediated superconductivity in graphene by lithium deposition. *Nat. Phys.* **2012**, *8*, 131−134.
(62) Ip, A. H.; Thon, S. M.; Hoogland, S.; Voznyy, O.; Zhitomirsky, D.; Debnath, R.; Levina, L.; Rollny, L. R.; Carey, G. H.; Fischer, A.; et al. Hybrid Passivated Colloidal Quantum Dot Solids. *Nat. Nanotechnol.* **2012**, *7*, 577−582.

https://doi.org/10.1021/acs.nanolett.2c03427
Nano Lett. 2022, 22, 10224−10231